scientific reports

Check for updates

OPEN

Structure of ^{3}He

P. D. Morley

Using electron scattering data, the diffraction pattern off ^{3}He shows it to be an equilateral triangle possessing dihedral D_3 point group symmetry (PGS). Previous work showed that ^{4}He is a 3-base pyramid with C_{3v} PGS. ^{6}Li is predicted to have C_{2v} PGS. As nuclear $A \rightarrow$ large, atomic nuclei enter into the 'protein folding problem' with many possible groundstate PGS competing for lowest energy.

High energy elastic electron scattering off nuclei reveal diffraction patterns that characterize the internal nuclear structure. Using the diffraction data of[1,2], reference[3] showed that ^{4}He is a 3-base pyramid, having C_{3v} PGS. This finding is fatal for the nuclear shell model that **posits mean-field theory** and a $(1s)^4$ configuration (literally a sphere) for the α-particle. In reality, the atomic nucleus is a **true** many-body system, where each nucleon wavefunction depends critically on the position and spin of every neighbor. It can be argued that the many decades-old ^{3}He scattering data of[1,2] (recently joined by the data of[4] which agrees with the original data) is the most enigmatic nuclear scattering data ever obtained. Point group symmetry of small A nuclei is the key to the atomic nucleus. There exists Nuclear Physics Laboratories that have a *Mission Statement* to derive the atomic nucleus from Quantum Chromodynamics. After several decades of existence, they have not fulfilled their *Mission Statement*. This paper addresses some of their physics.

The experimenters themselves have compared the ^{3}He data to phenomenological theories and the reader is invited to see their short-comings. None of the published papers conceived that $A = 3$ nuclei have PGS, much less being an equilateral triangle. Reference[5] introduces three $^2S_{\frac{1}{2}}$, three $^2P_{\frac{1}{2}}$, one $^4P_{\frac{1}{2}}$ and three $^4D_{\frac{1}{2}}$ states that have specific wavefunctions chosen for their analytical tractability and physical plausiblity. Even so, the author had to exclude a region of configuration space in order to establish a 'hole'. The author calls this 'a three-nucleon repulsive core'. Technically, this paper has physics errors because it has cross-terms between the different irreducible representations of S_3. The final paper reviewed here is the calculation[6] of the ^{3}He form factor in the meson-exchange model. In the authors' words: 'The charge form factors show a striking disagreement with experiment: the theoretical momentum transfer at the first minimum is too high and the height of the second maximum is too low.' In addition, the famous 'hole' in the charge distribution for r = 0 is not reproduced. Of course, the meson-exchange model has other issues beyond the $A = 3$ system, but they will not be discussed. This concludes the short literature review. Here it is shown that ^{3}He is an equilateral triangle.

We calculate the charged form factor, $\tilde{F}_{ch}$, which in one-photon exchange, is

$$\tilde{F}_{ch}(q^2) = \int \rho(\mathbf{r}) \frac{\sin qr}{qr} d^3r \tag{1}$$

The nuclear charge density $\rho(\mathbf{r})$ for ^{3}He need not be spherically symmetric. The charge density for point nucleons is (τ_{3i} is the z-component isospin operator for nucleon numbered i)

$$\rho_{pt}(\mathbf{r}') = \int \Xi^*_{pt} \sum_{i=1}^{3} \frac{1}{2}(1 + \tau_{3i})\delta^3(\mathbf{r}' - \mathbf{r}_i)\Xi_{pt} d^3r_1 \ldots \tag{2}$$

Since the proton itself has charge density $\rho_p(r)$, then $\rho(\mathbf{r})$ is the convolution

$$\rho(\mathbf{r}) = \int \rho_{pt}(\mathbf{r}' - \mathbf{r})\rho(r')d^3r' \tag{3}$$

and now

$$\tilde{F}_{ch}(q^2) = \tilde{F}_{pt}(q^2)F_q(q^2) \tag{4}$$

where $\tilde{F}_{pt}(q^2)$ is the charge form factor using point nucleons and $F_q(q^2)$ is the Fourier transform of ρ_p which is the familiar dipole form factor[7] $(1 + q^2(.054842\text{fm}^2))^{-2}$. Experimentalists normalize the charge form factor by $F_{ch} = \tilde{F}_{ch}/Z$ (Z = nuclear charge) so the normalized $F_{ch}(0) = 1$; we will call the normalized charge form factor, 'the charged form factor'.

Blue Ridge Scientific LLC, Front Royal, VA 22630, USA. email: peter3@uchicago.edu

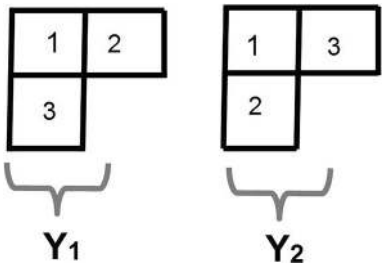

Figure 1. The standard Young Tableau generating the 2D IR of S_3.

We now construct $\Xi_{pt}(\mathbf{r}_1, \mathbf{s}_1, \mathbf{t}_1, \ldots)$ in which we indicate the position, spin and isospin variables. The S = 1/2, T = 1/2 supermultiplet has symmetry group S_3 irreducible representations (IR), due to the Pauli Principle. Furthermore, as explained below, Quantum Chromodynamics (QCD) requires that groundstate nuclei have PGS. The vertices of the lattice in the center-of-mass system are (c is the base)

$$\begin{aligned} \mathbf{a}_1 &= (0, 2\eta, 0) \\ \mathbf{a}_2 &= (c/2, -\eta, 0) \\ \mathbf{a}_3 &= (-c/2, -\eta, 0) \end{aligned} \tag{5}$$

If $\eta = c/(2\sqrt{3})$, the triangle is equilateral. The orientation of the lattice plane is immaterial, because the point-like charge density depends only on inner products $\mathbf{a}_i \cdot \mathbf{a}_j$ (due to the fact that the electron beam is not coherent). Using group theory[8], the ^{3}He point wavefunction Ξ_{pt} is made up of the three different IR $[\lambda]$ of S_3: the spatial symmetric Ψ_S 1D [3], the spatial anti-symmetric Ψ_A 1D $[1^3]$ and the mixed Ψ_M 2D [21].

$$\Xi_{pt}(\mathbf{r}_1, \mathbf{s}_1, \mathbf{t}_1, \ldots) = C_S \Psi_S + C_M \Psi_M + C_A \Psi_A \tag{6}$$

In Eq. (6), the C_i are constants. The reason for the decomposition is that the QCD Hamiltonian has effective nucleon $\mathbf{s}_i \cdot \mathbf{s}_j$ spin terms which mix the IR of S_3. For the basic spatial wavefunction, we take the zero phonon harmonic oscillator (H.O.). The harmonic oscillator parameter is the zero point energy (which is related to the Uncertainty Principle) of the nucleon in the atomic nucleus. We define $\phi(\mathbf{r}_1, \mathbf{r}_2, \mathbf{r}_3)$ to be

$$\phi(123) \equiv \phi(\mathbf{r}_1, \mathbf{r}_2, \mathbf{r}_3) = C^3 \prod_{i=1}^{3} exp[-(\mathbf{r}_i - \mathbf{a}_i)^2/\alpha^2] \tag{7}$$

where $C = \frac{1}{\alpha^{3/2}}(\frac{2}{\pi})^{9/4}$ and α is the H.O. length parameter. In Eq. (7), the '123' only reference the spatial variables $\mathbf{r}_1, \mathbf{r}_2, \mathbf{r}_3$. For simplicity of notation, hereafter, we put $\mathbf{a}_1 \equiv \mathbf{a}$, $\mathbf{a}_2 \equiv \mathbf{b}$, $\mathbf{a}_3 \equiv \mathbf{c}$. The spin-isospin wavefunction $ST(123)$ is

$$\begin{aligned} ST(123) \equiv &\frac{1}{2}[\chi(1)\uparrow \chi(2)\downarrow - \chi(2)\uparrow \chi(1)\downarrow]\chi(3)\uparrow \cdot \\ &[\tau(1)\uparrow \tau(3)\downarrow - \tau(3)\uparrow \tau(1)\downarrow]\tau(2)\uparrow \end{aligned} \tag{8}$$

where $\chi(2)\downarrow$ is nucleon 2 spin down, and $\tau(3)\uparrow$ is nucleon 3 isospin up (a proton). We now construct the individual wavefunctions of Eq. (6) by introducing the Young Tableau of Fig. 1 and the idempotent operators $\mathcal{A}, \mathcal{S}$ which respectively are the antisymmetrizer and symmetrizer. ^{3}He has positive parity, with P the parity operator.

$$\begin{aligned} \Psi_S &= \frac{1}{2}(1+P)\mathcal{S}[\phi(123)]\mathcal{A}[ST(123)] \\ \Psi_A &= \frac{1}{2}(1+P)\mathcal{A}[\phi(123)]\mathcal{S}[ST(123)] \\ \Psi_M &= \frac{1}{\sqrt{2}}[\Psi_1\tilde{\Psi}_1 - \Psi_2\tilde{\Psi}_2] \end{aligned} \tag{9}$$

where

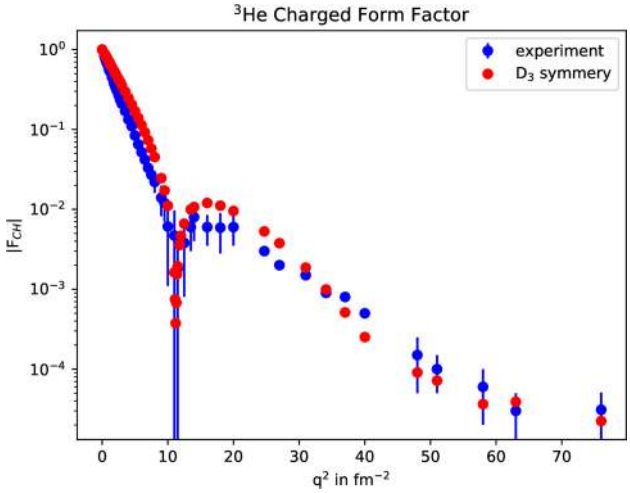

Figure 2. Equilateral triangle scattering of ^{3}He, using the one-photon approximation and neglecting neutron scattering.

$$\begin{aligned}\Psi_1 &= \frac{1}{2}(1+P)\frac{Y_1}{3}\phi(123)\\ \tilde{\Psi}_1 &= \frac{Y_2}{3}ST(123)\\ \Psi_2 &= \frac{1}{2}(1+P)\frac{Y_2}{3}(23)\phi(123)\\ \tilde{\Psi}_2 &= \frac{Y_1}{3}(23)ST(123)\end{aligned} \tag{10}$$

It is important for the reader to understand that in the 2D IR of S_3, a transposition operator such as (23) becomes a matrix in the configuration space spanned by the Young Tableau and the physical wavefunction is the antisymmetric $[1^3]$ component in the direct product of [21]⊗[21], Eq. (9). There are no cross-terms between the different IR in the calculation of Eq. (2). In conducting the research, one must construct master tables of matrix elements such as $ST(132)\tau_{32}ST(213) = -1/4$ and master tables of expectation values such as $\int \phi(213)P\phi(321)\delta^3(\mathbf{r}' - \mathbf{r}_2)d^3r_1d^3r_2d^3r_3 = C^2 exp\{-[(\mathbf{r}' - \mathbf{a})^2 + (\mathbf{r}' + \mathbf{b})^2]/\alpha^2\}exp\{-(\mathbf{b}+\mathbf{c})^2/2\alpha^2\}exp\{-(\mathbf{a}+\mathbf{c})^2/2\alpha^2\}$. Altogether, there are 36 + 36 + 192 terms in Eq. (2). The results in Fig. 2 are in good agreement with experiment, considering the one-photon scattering approximation and the neglect of neutron scattering.

In Table 1, we give the PGS parameters for ^{3}He and ^{4}He. Basically, the extra nucleon in ^{4}He sits on a withdrawn equilateral triangle base of ^{3}He. This is understandable because of the existence of a 4-body force in ^{4}He, discussed below. The radial (scalar) point nucleon nuclear density is

$$\rho_{pt}(r) = \frac{1}{4\pi}\int \rho_{pt}(\mathbf{r})d\Omega \tag{11}$$

which is displayed in Fig. 3. We see ^{3}He has a 'hole' at the center. Finally, we calculate the root-mean-squared R_{He} mass radius of ^{3}He, which is

$$R_{He} = \sqrt{< \Xi_{pt}|\sum_{i=1}^{3} r_i^2|\Xi_{pt} >} \tag{12}$$

This is done by assembling a master table of expectation values, such as $\int \phi(132)\sum_{i=1}^{3} r_i^2 P\phi(321)d^3r_1d^3r_2d^3r_3 = exp\{-(1/2\alpha^2)([\mathbf{b}+\mathbf{c}]^2 + [\mathbf{a}+\mathbf{c}]^2 + [\mathbf{b}+\mathbf{a}]^2)\}[\frac{9}{4}\alpha^2 + (\frac{\mathbf{a}-\mathbf{c}}{2})^2 + (\frac{\mathbf{a}-\mathbf{b}}{2})^2 + (\frac{\mathbf{b}-\mathbf{c}}{2})^2]$. The mass radius is the physical extent of the wavefunction (size of nucleus).

The atomic nucleus is the solution of the N-quark low energy semi-relativistic Hamiltonian. For N=3, reference[9] solved for the complete J^π N, Δ family using the 2-body charmonium potential[10]. (Recently, four-quark matter has been found, and it is anticipated it may have a PGS shape[11]. This further substantiates the Charmonium potential.) Kiefer was able to predict the known N, Δ J^π states and all the known photon decay amplitudes for transitions to the nucleon groundstate. Reference[12,13] solved the N = 6 quark problem and showed that the physical deuteron was due to quark-exchange Feynman diagrams. Reference[14] showed that the quark-exchange forces give rise to effective nucleon-nucleon potentials. Reference[15] showed that QCD has 2-, 3-, 4-body quark exchange forces. Finally, reference[16] was able to concatenate the N-quark Hamiltonian into a nuclear code. This showed that the atomic nucleus groundstate has PGS, while excitations are coherent (keeping the nuclear bonds intact: rotations and vibrations) and incoherent (breaking the nuclear bonds). The saturation of atomic forces is due to the fact that nucleons have only three quarks to exchange: the four-body quark exchange force, due to the

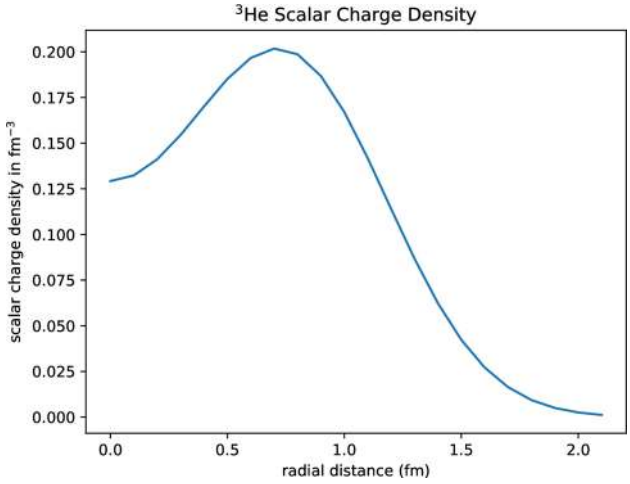

Figure 3. Scalar charge density of ^{3}He, showing the 'hole' at the center.

PGS parameters/results	^{3}He	^{4}He
% Spatial antisymmetric	None discernable	None discernable
% Spatial symmetric	15.99	13.6
% Spatial mixed	84.01	86.4
α^2 H.O. (fm^2)	0.644327	0.644327
3-Base length (fm)		1.341
Equilateral length (fm)	1.61	
Mass radius (fm)	2.023	1.79

Table 1. PGS comparison ^{3}He with ^{4}He.

gluon 4-body interaction, is the strongest binding mechanism for the atomic nucleus, reference[16]. The nuclear code can be expanded to predict groundstate spins, by noting that the 2-body, 3-body bonds are spin-dependent. For example, the binding energy of the A = 6 nucleus is $E(6) = E_4 + 2E_3 + 4E_2$, where E_i are the binding energies of the i-body bonds, so the E_2 spins cancel, leaving $2E_3$-spins ($J^\pi = 1^+$). Similarly, $E(7) = E_4 + 3E_3 + 4E_2$, with the E_2 spins canceling leaving $3E_3$ spins ($J^\pi = \frac{3}{2}^-$).

The key quantity allowing the nuclear interactions to occur is the overlap of nucleon wavefunctions in the atomic nucleus. There are two radii for the nucleon: the electromagnetic and the mass. For the nucleon in the S = T = 1/2 state, the former radius-squared is r^2_{Q-N}

$$r^2_{Q-N} =< \frac{1}{2}\frac{1}{2}\left|\sum_{i=1}^{3}\left(\tau_{3i}+\frac{1}{6}\right)r_i^2\right|\frac{1}{2}\frac{1}{2} > \tag{13}$$

which is a negative value for the neutron. Physically speaking, the electromagnetic radius measures the internal charge distribution while the mass radius r_M

$$r^2_M =< \frac{1}{2}\frac{1}{2}\left|\sum_{i=1}^{3} r_i^2\right|\frac{1}{2}\frac{1}{2} > \tag{14}$$

measures the physical size. In realty, the neutron mass radius and the proton mass radius are nearly identical in value because the gluons in Quantum Chromodynamics do not couple to electric charge. The mass radius of the nucleon is[9] $\sim 1.38-1.40$ fm, showing that the atomic nucleus has overlaping nucleon wavefunctions, allowing QCD color interactions to occur between colorless hadrons. An important experiment that can be conducted is high-energy elastic scattering off ^{6}Li, which is predicted to have C_{2v} PGS, reference[16]. However, as the nuclear $A \rightarrow$ large, it becomes very difficult to ascertain the geometry of the groundstate wavefunction, the 'protein folding problem'. For large A nuclei, one must consider that the Jahn-Teller effect[17] may appear, changing the assumed PGS.

Received: 23 April 2021; Accepted: 2 September 2021
Published online: 23 September 2021

References

1. McCarthy, J. S., Sick, I. & Whitney, R. R. Electromagnetic structure of the helium isotopes. *Phys. Rev. C* **15**, 1396 (1977).
2. Arnold, R. G. *et al.* Elastic electron scattering from ^{3}He and ^{4}He at high momentum transfer. *Phys. Rev. Lett.* **40**, 1429 (1978).
3. Morley, P. D. & Williams, S. A. On the structure of the alpha particle. *Z. Phys. A (Atomic Nuclei)* **331**, 239 (1988).
4. Camsonne, A. *et al.* JLab measurements of the ^{3}He form factors at large momentun transfers. *Phys. Rev. Lett.* **119**(16), 162501 (2017).
5. Schiff, L. I. Theory of the electromagnetic form factors of ^{3}H and ^{3}He. *Phys. Rev.* **133**, B802 (1964).
6. Coelho, H. T., Das, T. K. & Fabre de la Ripelle, M. Effect of two-pion exchange three-nucleon forces on trinucleon bound states. *Phys. Lett.* **109B**, 255 (1982).
7. Perdrisat, C. F. *et al.* Nucleon electromagnetic form factors. *Prog. Part. Nucl. Phys.* **59**, 694 (2007).
8. Hammermesh, M. *Group Theory and Its Application to Physical Problems* (Addison-Wesley, 1962).
9. Kiefer, M. L. Nonstrange Baryon Properties from One-Gluon Exchange and Linear Confinement Between Quarks. Ph.D. dissertation, Iowa State University (1983).
10. Politzer, H. D. Asymptotic freedom: An approach to strong interactions. *Phys. Rep.* **14C**, 129 (1974).
11. Liu, Z. Four-quark matter—A new era of spectroscopy. *AAPPS Bull.* **31**(1), 8 (2021).
12. Morley, P. D., Pursey, D. L. & Williams, S. A. Constituent quark model of the nucleon–nucleon interaction. *Phys. Rev. C* **42**, 2698 (1990).
13. Williams, S. A., Margetan, F. J., Morley, P. D. & Pursey, D. L. Application of the constituent quark nucleon–nucleon interaction to the deuteron. *Phys. Rev. C* **42**, 2711 (1990).
14. Reed-Margeton, D. A Local Approximation of a QCD-Inspired Nucleon–Nucleon Interation. Ph.D. dissertation, Iowa State University (1983).
15. Gleeson, A., Plümer, M. & Morley, P. D. Multibody quark forces in quantum chromodynamics. *Phys. Rev. D* **36**, 2575 (1987).
16. Morley, P. D. & Williams, S. A. Multiquark Hamiltonian and the nuclear force. *Z. Phys. A (Atomic Nuclei)* **336**, 321 (1990).
17. Jahn, H. A. & Teller, E. Stability of polyatomic molecules in degenerate electronic states. 1. Orbital degeneracy. *Proc. R. Soc. Lond. Ser. A Math. Phys. Sci.* **161**, 220–235 (1937).

Author contributions

All material is original by the author.

Competing interests

The author declares no competing interests.

Additional information

Correspondence and requests for materials should be addressed to P.D.M.

Reprints and permissions information is available at www.nature.com/reprints.

Publisher's note Springer Nature remains neutral with regard to jurisdictional claims in published maps and institutional affiliations.

Open Access This article is licensed under a Creative Commons Attribution 4.0 International License, which permits use, sharing, adaptation, distribution and reproduction in any medium or format, as long as you give appropriate credit to the original author(s) and the source, provide a link to the Creative Commons licence, and indicate if changes were made. The images or other third party material in this article are included in the article's Creative Commons licence, unless indicated otherwise in a credit line to the material. If material is not included in the article's Creative Commons licence and your intended use is not permitted by statutory regulation or exceeds the permitted use, you will need to obtain permission directly from the copyright holder. To view a copy of this licence, visit http://creativecommons.org/licenses/by/4.0/.

© The Author(s) 2021